Horm Mol Biol Clin Invest 2012;10(1):217–225 © 2012 by Walter de Gruyter • Berlin • Boston. DOI 10.1515/hmbci-2012-0006

From tissue invasion to glucose metabolism: the many aspects of signal transducer and activator of transcription 3 pro-oncogenic activities

Sara Pensa[1,a], Marco Demaria[2,a], Lidia Avalle[3], Isaia Barbieri[4], Annalisa Camporeale[3] and Valeria Poli[3,*]

[1] Department of Pathology, University of Cambridge, Cambridge, UK
[2] Buck Institute for Research on Aging, Novato, CA, USA
[3] Molecular Biotechnology Center and Department of Genetics, Biology and Biochemistry, University of Turin, Turin, Italy
[4] Gurdon Institute, Cambridge, UK

Abstract

Background: The pro-oncogenic transcription factor STAT3 is constitutively active in tumours of many different origins, which often become addicted to its activity. STAT3 is believed to contribute to the initial survival of pre-cancerous cells as well as to hyper-proliferation and, later, metastasis.
Materials and methods: To evaluate the contribution of enhanced STAT3 activation in a controlled model system, we generated knock-in mice in which a mutant constitutively active *Stat3C* allele replaces the endogenous wild-type allele and analysed its contribution to breast tumorigenesis. Moreover, we generated Stat3$^{C/C}$ MEF cells and analysed their gene expression and metabolic profiles.
Results: Constitutively active STAT3 could enhance the tumorigenic power of the rat *Neu* oncogene in MMTV-Neu transgenic mice and trigger the production of earlier onset and more invasive mammary tumours. Tumour-derived cell lines displayed higher migrating, invading and metastatic ability and showed disrupted distribution of cell-cell junction markers. These features were mediated by STAT3-dependent over-expression of the C-terminal tensin-like (Cten) focal adhesion protein. Moreover, STAT3C alone was able to induce aerobic glycolysis and down-regulate mitochondrial activity, both in primary fibroblasts and in STAT3-dependent tumour cell lines, acting via both HIF-1α-dependent and independent mechanisms.
Conclusions: STAT3 can induce a metabolic switch that predisposes cells to aberrant survival, enhanced proliferation and, finally, tumour transformation. Later, enhanced Cten expression contributes to tissue infiltration and metastasis. While not excluding the contribution of many other tumour-specific STAT3 target genes, our data provide a unifying explanation of several pro-oncogenic STAT3 activities.

Keywords: aerobic glycolysis; breast tumours; Cten; STAT3; Warburg effect.

Introduction

STAT3, a member of the signal transducers and activators of transcription (STAT) family, is constitutively activated by phosphorylation on tyrosine 705 (Y-P) in a high percentage of tumours and tumour-derived cell lines of both liquid and solid origin. This factor is activated downstream of cytokines, growth factors and oncogenes including c-Src, EGFR and ErbB-2 [1]. STAT3 can also be phosphorylated on serine 727 (S-P) upon a number of stimuli leading to the activation of MAP kinases including Ras signalling [2]. Tumour cells often become addicted to STAT3, as interference with its transcriptional activity often triggers growth arrest and/or cell death. Indeed, STAT3 is required for cell transformation downstream of several oncogenes, the prototype being v-Src [3], which triggers STAT3 Y-P. Recently, STAT3 S-P induced by activated Ras was shown to trigger tumour transformation, driving STAT3 to localise to mitochondria and regulate cellular respiration [4, 5]. This non-canonical activity is required for Ras-dependent oncogenic transformation. Thus, STAT3 appears to play a central role in mediating tumour transformation downstream of many different oncogenes and growth factors, via both canonical transcriptional functions and non-canonical, non-nuclear activities.

The pro-oncogenic role of STAT3 in vivo is underlined by the ability of its constitutively active mutant form STAT3C [6] to enhance the malignant progression of skin tumours or to trigger the onset of lung adenocarcinomas [7] when over-expressed. STAT3 can contribute to tumorigenesis by enhancing tumour cell proliferation and survival, down-modulating anti-tumour immune responses, promoting angiogenesis and inducing cell movement and epithelial to mesenchymal transition (EMT) [8]. Moreover, it is considered one of the main factors mediating inflammation-induced cancer downstream of autocrine or paracrine production of IL-6 [9]. However, the mechanisms underlying in vivo STAT3 pro-oncogenic functions and the addiction of tumour cells are still incompletely understood. The STAT3-mediated gene expression signature varies in different tumour types, and many of its known pro-proliferative or anti-apoptotic target genes have been

[a] These authors contributed equally.
*Corresponding author: Dr. Valeria Poli, Molecular Biotechnology Center, Department of Genetics, Biology and Biochemistry, University of Turin, Via Nizza 52, 10126, Turin, Italy
Phone: +39 011 670 6428, Fax: +39 011 670 6432,
E-mail: valeria.poli@unito.it
Received February 10, 2012; accepted February 29, 2012; previously published online March 23, 2012

identified upon acute stimulation and are not consistently induced in tumours displaying lower but continuous STAT3 Y-P, which suggests distinct subsets of target genes.

We have recently generated knock-in mice in which a mutant *Stat3C* allele replaces the wild-type endogenous gene [10]. These mice display low but continuous STAT3 activity that is reminiscent of that observed in most STAT3-dependent tumour cells, and they represent a good model to assess STAT3 in vivo pro-oncogenic activities. Here, we present and discuss some of the most significant results. In particular, we show that STAT3 enhances tumour cell motility and invasion via a novel target gene, Cten, which represents a point of convergence with EGFR/HER2 signalling. Moreover, we discuss data showing that STAT3 acts as a master regulator of glucose metabolism and cellular respiration and that its inhibition leads to apoptotic death of STAT3-dependent cancer cells, at least partly via modifying their metabolic requirements [11].

Results

Stat3C mice display constitutive STAT3 nuclear localisation, Y-P and transcriptional activity

The *Stat3C* allele was expressed at physiological levels in all tissues analysed [10]. $Stat3^{C/C}$ mice died at a young age upon developing auto-immune myocarditis (A.C. and V.P., manuscript in preparation), whereas heterozygous $Stat3^{C/WT}$ mice were viable and fertile. STAT3C was indeed weekly constitutively active and showed slightly enhanced nuclear localization, Y-P and transcriptional activity in several tissues. Moreover, Y-P and nuclear localisation were prolonged in mouse embryonic fibroblasts (MEFs) or in the liver of $Stat3^{C/C}$ mice upon LPS or IL-6 treatment, respectively [10]. Both the transcriptional activity and DNA binding affinity of the STAT3C protein were comparable to those of the wild-type form, as judged by similar induction levels of tested target genes and by EMSA competitions (not shown). The slightly increased basal activity of STAT3C and its prolonged activation upon cytokine stimulation suggest a lower activation threshold and represent an ideal model to investigate STAT3 oncogenic functions in vivo.

STAT3C expression enhances Neu-mediated mammary gland tumorigenesis

Spontaneous tumour onset could not be assessed in ageing $Stat3^{C/C}$ mice due to their early mortality. No preneoplastic lesions or spontaneously arising tumours were detected in heterozygous $Stat3^{C/WT}$ mice up to 24 months of age, and mammary gland morphology was normal in virgin, pregnant and lactating $Stat3^{C/WT}$ female mice (I.B. and V.P., unpublished results). We therefore decided to assess potential cooperation with the *Neu* oncogene in mammary tumorigenesis in heterozygosity. MMTV-Neu transgenic mice (NeuT), which develop multiple foci of atypical hyperplasia progressing to invasive metastasizing carcinoma by 22–27 weeks, were intercrossed with $Stat3^{C/WT}$ mice to obtain NeuT, $Stat3^{C/WT}$ (N-C) or NeuT, $Stat3^{WT/WT}$ (N-WT) mice [10]. N-C mice developed palpable tumours significantly earlier than their N-WT control littermates (Figure 1A, p=0.0014). N-C tumours showed normal proliferation rates, as assessed by PCNA staining, but sensibly reduced TUNEL-positive apoptotic nuclei (not shown). The main biochemical pathways involved in Neu-mediated mammary tumorigenesis were unaffected (data not shown).

Three independent cell lines were derived from tumours of each genotype and named C or WT 1, 2 or 3. All three C cell lines displayed increased nuclear, phosphorylated STAT3, which suggests enhanced activity of the *Stat3C* allele. However, no significant differences were detected in Pten, Akt, Gsk3-β, Src and Erk expression or activation levels (not shown). Likewise, C and WT cell lines did not differ significantly in terms of proliferation or resistance to starvation-mediated apoptosis (data not shown). These results are not surprising, although they are in apparent contradiction with the observed reduced apoptotic index of the N-C tumours, as in vitro stabilisation of tumour cells involves the selection of cells able to survive and can thus mask original features. In contrast, marked differences in cell morphology and cell contact organization were evident. All WT cell lines displayed a well differentiated epithelial phenotype growing in tight islets with well organised and continuous adherent and tight junctions, as shown by staining of E-Cadherin, β-Catenin and Zonula occludens-1 (Zo-1) (Figure 1B). Accordingly, actin fibres were primarily located in the cortical region. In contrast, despite similar expression levels detected by Western blot (not shown), all C cell lines displayed discontinuous E-Cadherin, β-Catenin and Zo-1 distribution, reduced cortical actin and evident actin stress-fibres that were not detected in the WT cells (Figure 1B).

Migration and extra-cellular matrix invasion of the C and WT cell lines were assessed by Transwell assays with or without a Matrigel coating (Figure 2A). Migration was at least doubled in all C cell lines (p=0.0013), which also showed significantly enhanced Matrigel invasion potential (p=0.03). These results suggest higher invasive and metastatic activity. To evaluate these parameters in vivo, C1 or WT1 cells were injected intravenously into nude mice, and the formation of lung metastases was assessed after 3 or 5 weeks of injection. C1 cells produced significantly more and faster growing lung metastases (Figure 2B). Similar results were obtained with the other cell lines (not shown). C1 cells were also able to produce subcutaneous tumours displaying fast and regular growth and reaching 10-mm diameters after 5 weeks, whereas tumours produced by the WT1 cells grew much slower and never reached a 10-mm size (not shown).

Cten is a novel STAT3 target gene partly mediating cell contact disruption and enhanced migration

Gene expression profiles of all cell lines were compared using an Illumina microarray platform. The "rank products" function was used to produce a list of 23 up-regulated genes, most of which were functionally related to growth control and/or tumour biology [10]. Consistent differential expression was confirmed for Cten/tensin 4, Galectin 3 (Lgals3), Twist1, Lypd3 (ly6/Plaur domain containing 3) and Proliferin 2.

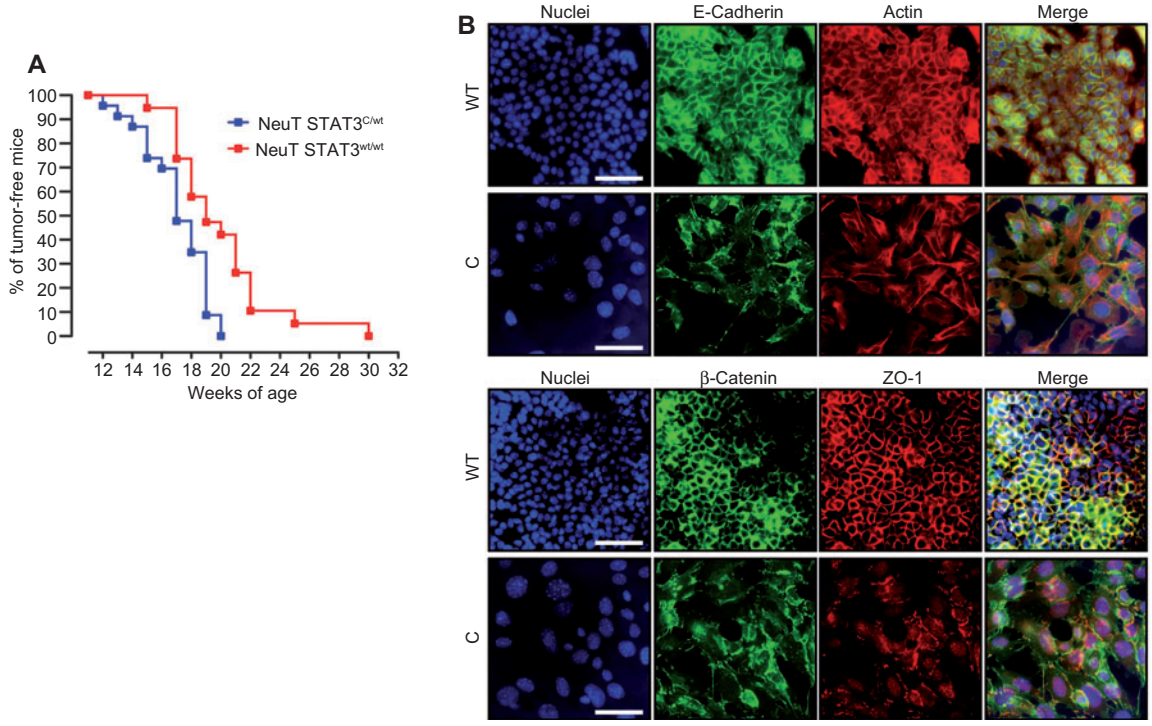

Figure 1 Stat3C enhances Neu-mediated mammary gland tumorigenesis.
(A) Kaplan-Meier curves showing the percentage of N-WT (n=20) or N-C (n=24) female mice free of palpable tumours as a function of age (p=0.0014). (B) The C1 and WT1 tumour-derived cell lines were plated on coated glass slides and incubated with phalloidin-TRITC or with antibodies against E-Cadherin, β-Catenin (mouse monoclonal) or Zo-1 (rabbit polyclonal) followed by Hoechst staining and incubation with FITC-labelled anti-mouse or TRITC-labelled anti-rabbit antibodies. Modified from reference [10].

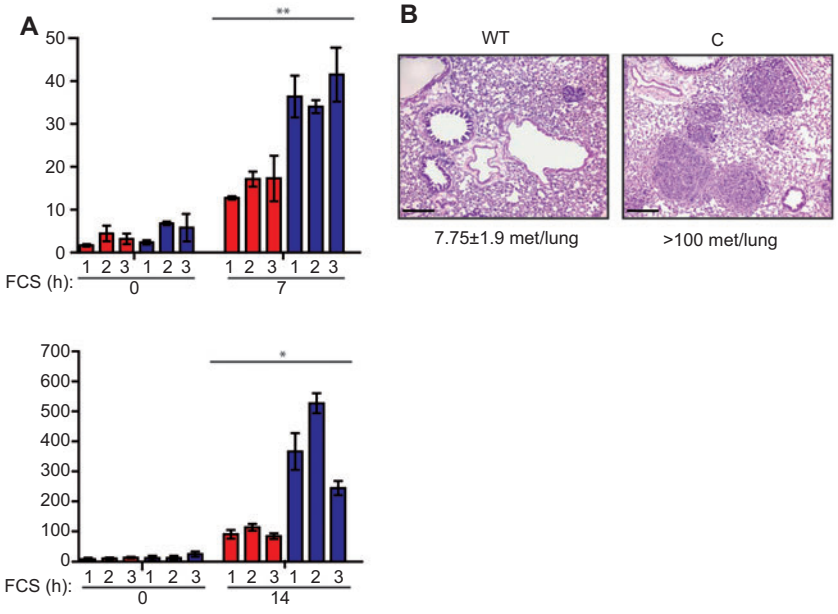

Figure 2 C cell lines display increased invasivity, both in vitro and in vivo.
(A) The indicated tumour-derived cell lines were subjected to Transwell migration assay (top) or to Matrigel invasion assay (bottom) in response to FCS. The histograms (C, blue bars; WT, red bars) show the mean number±SEM of migrated cells per microscopic field (20X, p=0.0013), or the mean number±SEM of invading cells per Transwell insert expressed as a percentage of the value obtained with WT1 stimulated cells (p=0.003). One representative experiment out of three independently performed in triplicate is shown in each case. (B) In vivo tumorigenesis: 1×10^5 WT1 or C1 cells were injected in the tail vein of nude mice (n=4), and the lungs were dissected 3 weeks after injection, fixed, sectioned and stained with H&E (scale bar=1 mm). The mean number of metastases per lung is shown. Modified from reference [10].

In addition, both Cten and Twist 1 also displayed significantly higher expression in the N-C tumours as compared to their N-WT controls (not shown).

Cten, the most consistently up-regulated gene, has been shown to be implicated in EGF-dependent mammary cell migration [12]. We therefore decided to assess its contribution to the observed phenotype of the C cell lines. siRNA treatment could efficiently reduce Cten levels to about 20% in both the C1 and C2 cell lines (not shown), resulting in significant inhibition of cell migration (Figure 3A) and, intriguingly, in partial reversion of both Zo-1 and β-Catenin cell surface distribution (Figure 3B). Cells adopted a more epithelial phenotype and displayed enhanced and more continuous cortical localisation of both epithelial markers, which correlates with tighter cell-cell contact, as evident in the phase-contrast images.

Both Cten overexpression and increased cell migration were indeed dependent on Stat3 activity, as treatment of C1 cells with the specific Stat3 inhibitor S3I coordinately and strongly reduced Stat3 phosphorylation, Cten levels and cell migration (Figure 3C). In addition, we observed that IL-6 treatment could efficiently upregulate Cten in MCF10 human mammary cells in a STAT3-dependent manner [10].

STAT3 constitutive activation elicits pre-oncogenic features in *Stat3$^{C/C}$* MEFs

We sought then to assess whether primary *Stat3$^{C/C}$* MEFs displayed pre-oncogenic or transformed features [11]. *Stat3$^{C/C}$* cells grew faster than their wild-type controls and displayed an accelerated cell cycle, with a more rapid transit through S-phase (not shown). Despite growing in monolayer, they reached higher cell density at confluence and were highly resistant to apoptosis induced by different stimuli, such as H_2O_2 treatment (20% of apoptotic cells after 16 h, compared to 85% in the wild-type controls, Figure 4A), serum starvation and UV treatment [11]. Moreover, *Stat3$^{C/C}$* cells

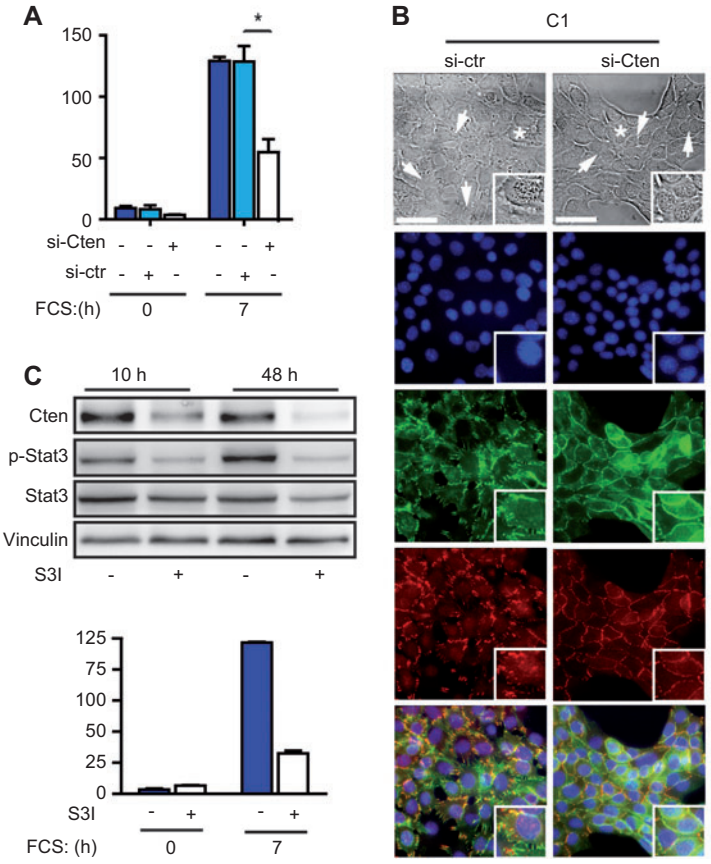

Figure 3 Cten silencing partially reverts the aggressive phenotype of C cells.
(A, B) C1 cells were treated for 72 h with the SMARTpool siRNA reagent (Accell system, Dharmacon) against Cten (si-Cten) or with a control Accell non-targeting siRNA (si-ctr) and subjected to a Transwell migration assay in response to FCS (A) or to immunofluorescence staining (B). (A) Values are shown as mean numbers±SEM of migrated cells per microscopic field (20X) of triplicates in one representative experiment out of two independently performed ($p<0.05$). (B) Phase contrast and immunofluorescence images of silenced C1 cells from (A). Arrows in the phase contrast images indicate particularly evident discontinuous (si-ctr) vs. tight (si-Cten) cell-cell contacts. Nuclei are shown in blue, β-Catenin in green, Zo-1 in red. The areas indicated by an asterisk in the phase contrast images are magnified in the insets (4× magnification). Scale bar=20 μm. (C) C1 cells were treated or not with the Stat3-specific inhibitor S3I for 10 or 48 h and analysed by Western blot with the indicated antibodies (top) or treated for 48 h, followed by Transwell migration assay in response to FCS (bottom). Modified from reference [10].

showed a strong delay in spontaneous senescence, as shown by β-galactosidase staining 3 and 6 weeks post-confluence (Figure 4B). Whereas all *Stat3*$^{WT/WT}$ cells were dead by 6 weeks, *Stat3*$^{C/C}$ cells began to show β-gal positivity but were able to survive and resume proliferation when passaged.

Stat3C induces a metabolic switch to aerobic glycolysis in primary MEFs

Gene expression profiling revealed about 1000 differentially expressed genes between *Stat3*$^{C/C}$ and *Stat3*$^{WT/WT}$ MEFs. Many of the down-regulated genes in the *Stat3*$^{C/C}$ cells belonged to gene ontology (GO) categories related to mitochondrial function (not shown). Conversely, several genes involved in glycolysis were highly expressed in the *Stat3*$^{C/C}$ cells, including the hypoxia inducible factor (Hif)-1α and the pyruvate dehydrogenase kinase (Pdk)-1, the glucose transporter Glut-1 and two key enzymes, phospho-fruktokinase L-type (Pfk-L) and enolase-1 (Eno-1), all of which are known HIF-1α target genes (Figure 5A). Accordingly, *Stat3*$^{C/C}$ cells exhibited a glycolytic phenotype, producing higher amounts of lactate and consuming more glucose (Figure 5B), and they were highly sensitive to glucose deprivation as compared to their wild-type controls, as shown by both cultivating cells in a glucose-free medium and by treatment with the glucose analog 2-DG [11].

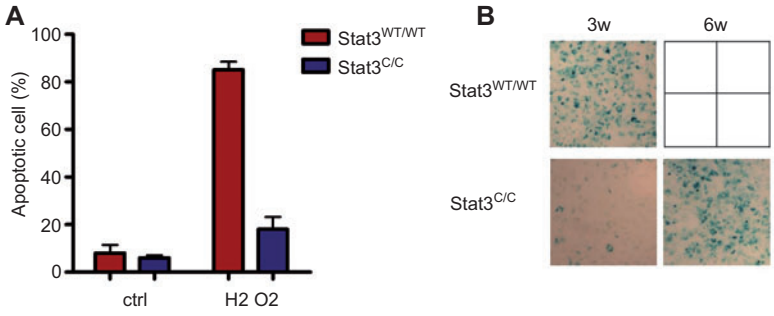

Figure 4 Phenotype of the *Stat3*$^{C/C}$ MEFs.
Primary MEFs were derived from *Stat3*$^{C/C}$ or *Stat3*$^{WT/WT}$ embryos, and experiments were performed on at least three independent samples per genotype. (A) Apoptosis protection. Cells were treated with H_2O_2 for 16 h, and stained with Annexin V. Numbers represent the percentage± SEM of Annexin V positive cells. (B) Delayed senescence. β-galactosidase activity assessed at 3 and 6 weeks post-confluence. *Stat3*$^{WT/WT}$ cells were all dead at 6 weeks. Modified from reference [11].

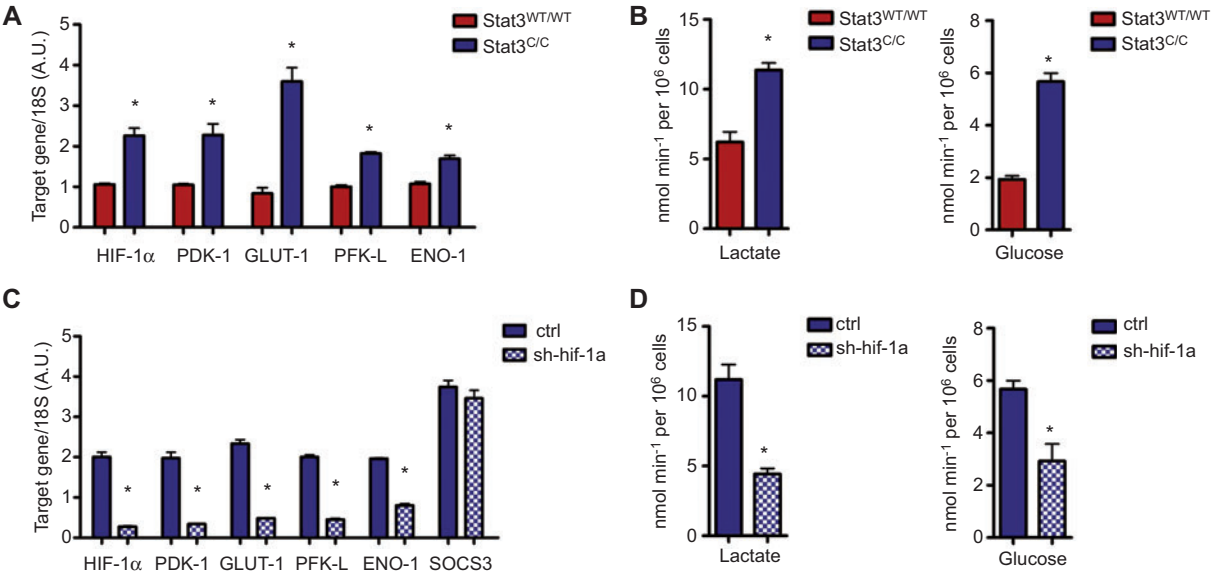

Figure 5 HIF-1α dependent glycolytic metabolism of *Stat3*$^{C/C}$ MEFs.
The histograms represent mean values±SEM of three independent experiments. *p≤0.01. (A) Taqman RT-PCR quantification of HIF-1α, hypoxia-inducible factor-1α; PDK-1, pyruvate dehydrogenase kinase-1; GLUT-1, glucose transporter-1; PFK-L, phospho-fruktokinase-liver type; ENO-1, enolase-1. (B) Lactate production was measured in the culture medium as a function of concentration, time and cell number. Glucose intake was calculated as the difference in glucose concentration in the medium before and after cell culturing. TaqMan RT-PCR quantification of the indicated mRNAs (C), lactate production and glucose intake (D) were measured in cells either silenced or not for HIF-1α (sh-Hif-1a). Modified from reference [11].

Hif-1α silencing normalised the glycolytic metabolism of *Stat3*$^{C/C}$ MEFs, which led to down-regulation of Pdk-1, Glut-1, Pfk-L and Eno-1 mRNAs, but not of the glycolysis-unrelated STAT3 target Socs3 (Figure 5C). Accordingly, lactate production, glucose intake and sensitivity to glucose deprivation were strongly reduced (Figure 5D and not shown). Thus, the expression of STAT3C, which mimics the constitutive STAT3 activation observed in many tumours, is sufficient to promote aerobic glycolysis, acting at least in part through the transcriptional induction of HIF-1α.

Reduced mitochondrial activity in *Stat3*$^{C/C}$ MEFs

Stat3$^{C/C}$ MEFs exhibited a significant down-regulation of nuclear-encoded genes involved in mitochondrial function, which correlates with reduced protein levels of representative components of the electron transport chain (ETC), particularly those belonging to complexes IV and V (Figure 6A). This observation suggests potentially reduced cellular respiration, similar to what was observed in cancer cells displaying aerobic glycolysis and the Warburg effect. We thus assessed both mitochondrial-specific Ca^{2+} uptake, which directly regulates oxidative phosphorylation, and mitochondrial ATP production. *Stat3*$^{C/C}$ MEFs indeed showed reduced mitochondrial Ca^{2+} uptake upon ATP stimulation (Figure 6B). Accordingly, both mitochondrial ATP production and basal respiratory chain activity were reduced (Figures 6C and 6D), which correlated with lowered maximal respiratory chain activity measured in the uncoupled state (Figures 6E). Importantly, the reduced mitochondrial activity was STAT3-dependent but could not be rescued by Hif-1α silencing (not shown), which suggests that constitutively active STAT3 regulates aerobic glycolysis and cellular respiration via two distinct mechanisms.

STAT3-dependent glycolysis contributes to in vitro and in vivo survival of cancer cell lines addicted to STAT3 activity

Our data suggest that constitutively active STAT3 can act as a central mediator of aerobic glycolysis, which would explain the general STAT3 addiction of cancer cells. To test this idea, we assessed the effects of inhibiting STAT3 on the glycolytic metabolism and mitochondrial activity of the STAT3-dependent epithelial tumour cell line MDA-MB468. Inhibition of STAT3 activity with the S3I compound dramatically lowered Hif-1α and Pdk-1 expression and decreased lactate production (Figure 7A), while rescuing mitochondrial-Ca^{2+} uptake at the same time [Figure 7B). Similar observations were obtained with other two STAT3-dependent cell lines (DU145 and SKBR3). STAT3 inhibition did not have any effects on the control cancer cell line T47D, which does not display constitutive STAT3 activity and, accordingly, does not depend on STAT3 for survival (data not shown). Thus, tumour cell lines that display constitutive STAT3 Y-P and are dependent on STAT3 for survival exhibit a strictly

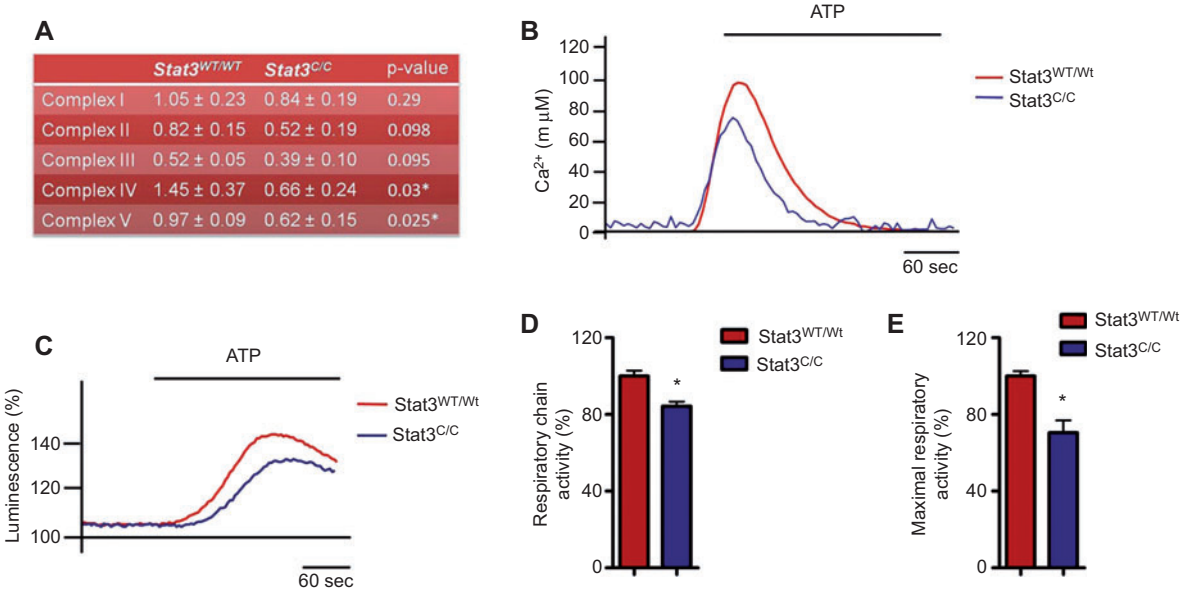

Figure 6 Decreased mitochondrial activity of *Stat3*$^{C/C}$ MEFs. (A) Mitochondrial complexes were quantificated by Western blot. The following antibodies against specific ETC components were used: CI subunit NDUFB8, complex I; CII-30kD, complex II; CIII-Core protein, complex III; CIV subunit, complex IV; CV alpha subunit, complex V. Actin and SOD2 were used as internal controls for total and mitochondrial content, respectively. (B) Mitochondrial Ca^{2+} homeostasis. MEFs of the indicated genotypes were transduced with a mitochondria-targeted aequorin construct; light emission was measured upon challenging with 100 µM ATP as indicated. (C) ATP-induced changes in ATP concentration in mitochondria. MEFs were transiently transfected with a mitochondria-targeted luciferase construct 36 h prior to ATP stimulation and luciferase measurement. Data are expressed as a percentage of the initial value. (D) Respiratory chain activity measured with resazurine. (E) Maximal respiratory chain activity, measured with the use of resazurine in the presence of 300 nM FCCP. *p<0.01. Modified from reference [11].

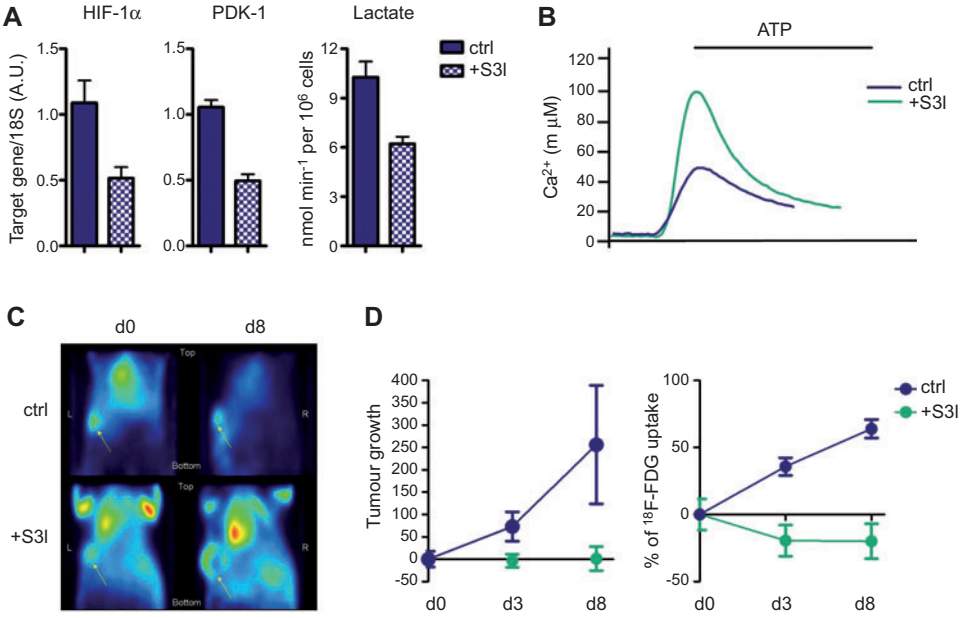

Figure 7 In vitro and in vivo STAT3-dependent glycolytic metabolism in MDA-MB468 human breast tumour cells. (A) Expression of the indicated mRNAs and lactate production were measured in MDA-MB468 cells, either treated or not with the S3I STAT3 inhibitor for 12 h. (B) The mitochondrial Ca^{2+} response was assessed as described in the legend to Figure 6, in cells either treated or not with S3I for 12 h. (C) Tumour ^{18}F-FDG uptake. Inoculated MDA-MB468 tumours were left to grow up to 60 mm^3 prior to S3I treatment, followed after 3 and 8 days by ^{18}F-FDG injection. Images were acquired at the indicated times after the first S3I treatment. Shown are tumour coronal sections of one (out of five) S3I-treated (8 days) and one (out of three) control mice. Yellow arrows indicate the tumours. (D) Left, mean tumour volume±SEM at 3 and 8 days after S3I treatment. Right, variation of glucose uptake normalised over tumour size at the indicated times. % of ^{18}F-FDG uptake=$(Suv_{d=n}–Suv_{d=0})*100/Suv_{d=0}$. Modified from reference [11].

STAT3-dependent aerobic glycolytic phenotype, comparable to that observed in the *Stat3*$^{C/C}$ MEFs.

To confirm the fundamental role of STAT3 in regulating the glycolytic switch of STAT3-dependent tumour cells in vivo, we measured the glucose uptake of xenografted MDA-MB468 tumours in the presence or absence of S3I treatment by means of PET analysis, using the radioactive glucose-analogue ^{18}F-FDG (PET-FDG, Figure 7C). S3I treatment was started when the tumours reached the volume of 60 mm^3 (day 0). Tumours of untreated mice continued to grow, displaying increasingly high ratios between glucose uptake and tumour volume (Figure 7D). In contrast, tumour growth in S3I-treated mice was arrested after three days of treatment, whereas the glucose uptake: tumour volume ratio decreased, which suggests that STAT3 addiction in these cancer cells is based at least partly on STAT3-dependent aerobic glycolysis.

Discussion

The addiction to STAT3 constitutive activity observed in many tumours of distinct origin, where distinct patterns of target genes are induced, suggests that tumour cells rely on STAT3 transcriptional activity for some fundamental biological function shared by most tumours. Additionally, STAT3 constitutive activity is often observed in sites of chronic inflammation as a result of localised production of IL-6, where it triggers the onset of inflammation-related cancer, often in conjunction with the transcription factor NF-kB [9]. Thus, STAT3 appears to act at different levels during tumorigenesis, by, i) altering the activity of the pre-tumoural niche; ii) favouring survival and abnormal proliferation during the transformation process and iii) enhancing the invasive and metastatic potential of fully transformed tumour cells.

Our data show indeed that constitutively active STAT3 can enhance breast tumorigenesis downstream of the *Neu* oncogene via protection from apoptosis and promotion of tumour aggressiveness and metastasis. Interestingly, dissection of the latter indicates that in the C and WT tumour-derived cell lines, the aggressive phenotype could correlate with disrupted distribution of adherent and tight junctions, loss of cortical actin and development of actin stress fibres, mediated for a good part by the newly identified STAT3 target Cten [13]. Cten is known to mediate EGF-induced migration [12], to promote cell motility of colon and pancreas cancer cells, and to be overexpressed in late stage epithelial tumours of different types, often correlating with STAT3 constitutive activity [14]. CTEN expression is particularly elevated in the highly aggressive and invasive inflammatory breast cancers, together with high EGFR and HER2 levels, loss of oestrogen receptor and lymph node metastasis [12]. Thus, our observation of STAT3-mediated CTEN induction by IL-6 suggests that this tensin may be an important mediator in the loop inflammation-STAT3-migration/metastasis, representing a point of convergence with altered EGFR and/or HER2-mediated signalling, both of which can trigger STAT3 activation.

We also show that constitutive STAT3 activity is sufficient to trigger the switch to aerobic glycolysis. This property can explain why so many biologically distinct tumours are addicted to STAT3 activity for continuous survival and growth. Indeed, most cancer cells share the feature of producing ATP, primarily through aerobic glycolysis, the so-called Warburg effect, thus becoming addicted to high glucose influxes [15]. Moreover, enhanced aerobic glycolysis can favour tumoral transformation. The central role of STAT3 in orchestrating this metabolic switch is corroborated by the observation that several STAT3-dependent tumour cell lines display high aerobic glycolysis mediated by STAT3 activity. STAT3 addiction in these cells is indeed linked to STAT3-induced glycolysis, as suggested by the observation that its inhibition down-regulates the glycolysis rate while up-regulating mitochondrial activity prior to leading to apoptotic cell death. Importantly, our data with tumour xenografts support the idea that STAT3 addiction also occurs via the same mechanism in vivo [11].

The mechanism of this STAT3-dependent metabolic switch appears to be twofold. Aerobic glycolysis is due to the low but continuous induction of HIF-1α mRNA (and protein) mediated by constitutive STAT3 activation. This sustained induction is likely to represent an important functional difference between acute and constitutive STAT3 activity and to allow fast proliferation [16]. However, the down-regulation of mitochondrial activity is HIF-1α-independent and is likely caused by the observed STAT3-dependent down-regulation of nuclear genes encoding for mitochondrial proteins, which leads to reduced levels of ETC components. The reduced mitochondrial activity may contribute to the decreased ROS accumulation observed in the *Stat3*$^{C/C}$ MEFs [11], which in turn is likely to trigger high resistance of these cells to apoptosis and senescence, two hallmarks of cellular transformation. Although *Stat3*$^{C/C}$ MEFs are not transformed, they present features of cells having undergone a first hit in the multi-step transformation process, as suggested by preliminary experiments with spontaneous immortalization [18].

In conclusion, we show here that STAT3, found constitutively active in the pre-tumoral niche, can induce a metabolic switch that predisposes cells to aberrant survival, enhanced proliferation and, finally, tumour transformation. Moreover, enhanced IL-6-induced Cten expression later contributes to tissue infiltration and metastasis. While not excluding the contribution of many other tumour-specific STAT3 target genes, we believe that this represents a unifying view explaining several of the pro-oncogenic activities of this multi-faceted transcription factor.

Materials and methods

Animals, treatments and analysis

Mice were maintained in the transgenic unit of the Molecular Biotechnology Center (University of Turin) under a 12-h light-dark cycle and provided food and water *ad libitum*. Procedures were conducted in conformity with national and international laws and policies as approved by the Faculty Ethical Committee. The generation of the N-C mice and the analysis of tumour onset were described [10].

Cell lines

Tumour cell lines were isolated from three different N-C and N-WT mice and cultured in complete medium as described [10]. MEFs were prepared from 13.5-day embryos. Both MEFs and MDA-MB468 (ATCC, Manassas VA, USA) were grown as described [11]. S3I-201 inhibitor was used at a concentration of 100 μM (MEFs and MDA-MB468) or 200 μM (C1 cells). Transwell invasion and migration assays were performed as described [10].

Lung metastasis

1×10^5 cells were injected into the tail vein of nude CD1 female mice. Mice were sacrificed after 3 weeks, and the lungs fixed as described [10]. Semiserial sections at 100-μm intervals were stained with H&E, and neoplastic lesions were counted in blind.

Cten silencing

Cells were plated at a density of 60% and incubated for 72 h with 1 μM Accell SMARTpool siRNA (E-054907-00) or with the Accell Non-Targeting siRNA (D-001910-01-05, Dharmacon, Thermo Fisher Scientific, Lafayette, CO, USA) according to the manufacturer's protocol.

Immunofluorescence

Immunofluorescence was performed as previously described [10] and imaged with an Axiovert 200M Zeiss microscope or an Axio-Observer-Z1 Zeiss microscope (Carl Zeiss, Inc., Oberkochen, Germany) with the ApoTome system for optical sectioning.

In vitro cell death and senescence assay

Cell death: cells were treated with H_2O_2 (Sigma Aldrich, St. Louis, MO, USA, 1 mM for 16 h) followed by staining with Annexin-V. Senescence: cells were stained at the indicated times after plating using a Senescence Cells Histochemical Staining Kit (Sigma Aldrich), according to the manufacturer's protocol.

Real time-PCR

Total RNA was prepared with the PureLink Micro-to-Midi total RNA Purification System (Invitrogen, Carlsbad, CA, USA). qRT-PCR reactions were performed as previously described [17] using the Universal Probe Library system (Roche Italia, Monza, Italy). The 18S rRNA pre-developed TaqMan assay (Applied Biosystems, Foster City, CA, USA) was used as an internal control.

Glucose and lactate measurements

Glucose or lactate was measured in cell supernatants 3 h after fluid replacement using a Glucose Assay Kit (Sigma Aldrich) or a Lactate Colorimetric Assay Kit (Abcam, Cambridge, UK). Data were normalised to cell counts.

Lentiviral infection

pLKO vectors carrying either scrambled or shRNA-Hif-1α sequences (Open Biosystems, Huntsville, AL, USA) were packaged by

transfecting 293T cells and used to infect cells for 24 h, followed by puromycin selection for 48 h.

Calcium and ATP measurements

Cells were grown on glass coverslips at 50% confluence. For Ca^{2+} measurements, cells were infected with the adenovirus expressing the appropriate aequorin chimera, and the light signal was collected and calibrated into [Ca^{2+}] values, as previously described [11]. For measuring mitochondrial ATP, MEFs were transfected with mitochondrial luciferase (mtLuc), and luminescence was measured after 36 h as described [11].

Respiratory chain activity

MEFs grown in 24-well plates were washed with PBS and PBS containing 5 mM glucose, and 6 μM resazurine was added and fluorescence was recorded immediately in a microplate reader (Infinite M200, Tecan, Austria) at 510-nm excitation and 595-nm emission wavelengths. For control of the threshold activity, cells were preincubated for 15 min with 2 μM KCN in complete medium, and measurements were performed as described above but in PBS containing 2 μM KCN. The activity values were normalised to mg of protein.

Small animal PET

PET images were acquired on the positron emission tomograph for small animals, the YAP-(S)PET system, as described [11]. Briefly, mice were anesthetised by inhalation of 2% of isofluorane and intravenously injected with 350μCi±50 of [^{18}F]fluorodeoxyglucose ([^{18}F]FDG) in a 0.15-mL volume. Quantitative image analysis of tracer uptake was evaluated by drawing the region of interest (ROI) of tumours on the transaxial images. [^{18}F]FDG uptake was quantified as standardised uptake values (SUV) and as a percentage of the injected dose per gram of tissue (%ID/g).

Statistical analysis

Kaplan-Meier survival curves were analysed by Prism4 (GraphPad software); p-values were calculated using the long-rank test. All other p-values were calculated using Student's t-test (unpaired, two tailed).

Acknowledgements

This work was supported by the Italian Cancer Research Association (AIRC IG9272) and the Italian Ministry for University and Research (FIRB and MIUR) to V.P.

References

1. Turkson J, Jove R. STAT proteins: novel molecular targets for cancer drug discovery. Oncogene 2000;19:6613–26.
2. Ceresa BP, Horvath CM, Pessin JE. Signal transducer and activator of transcription-3 serine phosphorylation by insulin is mediated by a Ras/Raf/MEK-dependent pathway. Endocrinology 1997;138:4131–7.
3. Bromberg JF, Horvath CM, Besser D, Lathem WW, Darnell JE Jr. Stat3 activation is required for cellular transformation by v-src. Molecular and cellular biology 1998;18:2553–8.
4. Wegrzyn J, Potla R, Chwae YJ, Sepuri NB, Zhang Q, Koeck T, Derecka M, Szczepanek K, Szelag M, Gornicka A, Moh A, Moghaddas S, Chen Q, Bobbili S, Cichy J, Dulak J, Baker DP, Wolfman A, Stuehr D, Hassan MO, Fu XY, Avadhani N, Drake JI, Fawcett P, Lesnefsky EJ, Larner AC. Function of mitochondrial Stat3 in cellular respiration. Science 2009;323:793–7.
5. Gough DJ, Corlett A, Schlessinger K, Wegrzyn J, Larner AC, Levy DE. Mitochondrial STAT3 supports Ras-dependent oncogenic transformation. Science 2009;324:1713–6.
6. Bromberg JF, Wrzeszczynska MH, Devgan G, Zhao Y, Pestell RG, Albanese C, Darnell JE Jr. Stat3 as an oncogene. Cell 1999;98:295–303.
7. Li Y, Du H, Qin Y, Roberts J, Cummings OW, Yan C. Activation of the signal transducers and activators of the transcription 3 pathway in alveolar epithelial cells induces inflammation and adenocarcinomas in mouse lung. Cancer Res 2007;67:8494–503.
8. Pensa S, Regis G, Boselli D, Novelli F, Poli V. STAT1 and STAT3 in tumorigenesis: two sides of the same coin? In: Stephanou A, editor. JAK-STAT pathway in disease. Austin: Landes Bioscience, 2009:100–21.
9. Bollrath J, Greten FR. IKK/NF-kappaB and STAT3 pathways: central signalling hubs in inflammation-mediated tumour promotion and metastasis. EMBO reports 2009;10:1314–9.
10. Barbieri I, Pensa S, Pannellini T, Quaglino E, Maritano D, Demaria M, Voster A, Turkson J, Cavallo F, Watson CJ, Provero P, Musiani P, Poli V. Constitutively active Stat3 enhances neu-mediated migration and metastasis in mammary tumors via upregulation of Cten. Cancer Res 2010;70:2558–67.
11. Demaria M, Giorgi C, Lebiedzinska M, Esposito G, D'Angeli L, Bartoli A, Gough DJ, Turkson J, Levy DE, Watson CJ, Wieckowski MR, Provero P, Pinton P, Poli V. A STAT3-mediated metabolic switch is involved in tumour transformation and STAT3 addiction. Aging (Albany NY) 2010;2:823–42.
12. Katz M, Amit I, Citri A, Shay T, Carvalho S, Lavi S, Milanezi F, Lyass L, Amariglio N, Jacob-Hirsch J, Ben-Chetrit N, Tarcic G, Lindzen M, Avraham R, Liao YC, Trusk P, Lyass A, Rechavi G, Spector NL, Lo SH, Schmitt F, Bacus SS, Yarden Y. A reciprocal tensin-3-cten switch mediates EGF-driven mammary cell migration. Nat Cell Biol 2007;9:961–9.
13. Lo SH, Lo TB. Cten, a COOH-terminal tensin-like protein with prostate restricted expression, is down-regulated in prostate cancer. Cancer Res 2002;62:4217–21.
14. Al-Ghamdi S, Albasri A, Cachat J, Ibrahem S, Muhammad BA, Jackson D, Nateri AS, Kindle KB, Ilyas M. Cten is targeted by Kras signalling to regulate cell motility in the colon and pancreas. PLoS One 2011;6:e20919.
15. Vander Heiden MG, Cantley LC, Thompson CB. Understanding the Warburg effect: the metabolic requirements of cell proliferation. Science 2009;324:1029–33.
16. Demaria M, Poli V. From the nucleus to the mitochondria and back: the odyssey of a multitask STAT3. Cell Cycle 2011;10:3221–2.
17. Schiavone D, Dewilde S, Vallania F, Turkson J, Di Cunto F, Poli V. The RhoU/Wrch1 Rho GTPase gene is a common transcriptional target of both the gp130/STAT3 and Wnt-1 pathways. Biochem J 2009;421:283–92.
18. Demaria M, Misale S, Giorgi C, Miano V, Camporeale A, Campisi J, Pinton P, Poli V. STAT3 can serve as a hit in the process of malignant transformation. Cell Deat Differ 2012; doi:10.1038/cdd.2012.20.